

Spatially regulated ubiquitin ligation by an ER/nuclear membrane ligase

Min Deng¹ & Mark Hochstrasser¹

The ubiquitin system targets many cellular proteins. Doa10 (also known as Ssm4), a yeast transmembrane ubiquitin ligase (E3), resides in the endoplasmic reticulum (ER), but it attaches ubiquitin to soluble proteins that concentrate in the nucleus. A central question is how nuclear substrates gain access to an enzyme in the ER. Here we show that Doa10 reaches the inner nuclear membrane. A subcomplex of nuclear pore subunits is important for this transport. Notably, another ER transmembrane E3, Hrd1 (also known as Der3), cannot localize efficiently to the inner nuclear membrane. Tethering Doa10 at the cell periphery inhibits degradation of soluble nuclear substrates but not cytoplasmic ones. If Doa10 is released from these peripheral sites, localization of Doa10 to the nuclear envelope and degradation of its nuclear substrates are restored in parallel. Thus, localization of Doa10 to the inner nuclear membrane is necessary for nuclear substrate degradation. These data indicate that different membrane ubiquitin ligases are spatially sorted within the ER–nuclear envelope membrane system and that this differential localization contributes to their specificity.

Protein degradation by the ubiquitin–proteasome pathway is responsible for most cellular protein turnover^{1–3}. Among the principal mediators of substrate specificity are the ubiquitin ligases (E3s), which, in conjunction with one or more specific ubiquitin-conjugating enzymes (E2s), recognize protein determinants called degradation signals or degrons⁴. Substrates are modified by ubiquitin or polymeric ubiquitin chains; polyubiquitin-modified proteins can then be recognized and degraded by the 26S proteasome³. Mammalian cells have hundreds of different E3s, whereas the model eukaryote *Saccharomyces cerevisiae* is estimated to have 60–100. E3s and E2s often localize to specific cellular compartments, and such compartmentalization can be a key component of their specificity⁵.

Doa10 is a conserved, 151-kDa integral membrane E3 with 14 transmembrane segments^{6,7}. Together with two ER-associated E2s, Ubc6 and Ubc7, Doa10 modifies a broad range of substrates, including ER membrane proteins, soluble nuclear proteins and soluble cytoplasmic substrates^{6,8,9}. One nuclear substrate, the Mat α 2 transcription factor, is targeted to the Doa10 pathway by its Deg1 degron^{8,10}. How Mat α 2 and other nuclear substrates gain access to the ER-localized Doa10 has remained a mystery. Either nuclear substrates are exported out of the nucleus to reach Doa10, or the E3 is transported to the inner nuclear membrane (INM) to reach its nuclear substrates (see Supplementary Fig. S1). As our preliminary data argued against the first possibility, we focused on investigating the latter hypothesis.

Targeted silencing indicates that Doa10 is in the INM

Immunogold electron microscopy was attempted for localizing Doa10–GFP (green fluorescent protein; Supplementary Fig. 2). Doa10–GFP, which is fully functional⁶, showed apparent localization to both sides of the nuclear envelope. However, endogenous Doa10 levels are very low, and only a few thin sections had bead distributions that appeared to show labelling on both the inner and outer nuclear envelope.

Given the limitations of these data, we developed two assays as alternatives to ultrastructural localization. The first was a ‘targeted silencing’ assay¹¹, which was initially designed to study the role of

nuclear localization in gene silencing. Here we adapted it to determine whether Doa10 expressed at endogenous levels could localize to the INM. The yeast silent mating-type locus gene silencer *HMR-E* contains three DNA elements (A, E and B), which recruit silencing factors (Fig. 1a). Deletion of any two elements leads to full de-repression of the *HMR* locus, but silencing is restored by anchoring the locus to the nuclear periphery where silencing factors are concentrated^{11,12}. By fusing the DNA-binding domain of Gal4 (G_{BD}) to Doa10, we measured potential INM tethering of an *HMR* derivative that had two silencing elements replaced by a triplicated Gal4-binding site (UAS_G). Expression of G_{BD} –Doa10 and endogenous Doa10 was similar (a 13 \times Myc epitope tag was appended to both) (Fig. 1b).

With an *hmr::TRP1* reporter, which allows gene expression to be measured by growth on medium lacking tryptophan, silencing was seen in the tester strain expressing G_{BD} –Doa10 (Fig. 1c, Supplementary Fig. 3). The effect was slightly less pronounced than with the positive control, overexpressed G_{BD} –Stt3 (ref. 11), but depended on the presence of the UAS_G sites and required at least one natural silencer sub-element as well as the Sir2 silencing factor (Supplementary Fig. 3). Therefore, G_{BD} –Doa10-mediated repression exhibited all the hallmarks of targeted silencing. We also detected specific binding of G_{BD} –Doa10 to the UAS_G sites in the modified *hmr::TRP1* locus by chromatin immunoprecipitation (Fig. 1d, lanes 1 and 2). These data indicate that Doa10 can reach the inner nuclear envelope.

Differential localization of ER membrane E3s

For a broader analysis of integral membrane protein localization to the INM, we developed a second, quantifiable cell-based assay that exploits the observation that increased expression of the Nup53 nucleoporin causes specific proliferation of the INM¹³. The resulting intranuclear membrane lamellae pack against the nuclear envelope (see Supplementary Fig. 2, right) and often also cut across the nuclear interior¹³. If Doa10 is in the INM, visualizing Doa10 in cells that overproduce Nup53 should reveal similar structures.

The *DOA10-GFP* strain was transformed with a *CUP1-NUP53* plasmid. After induction with copper, intranuclear lamellae were observed by electron microscopy. Both confocal (Fig. 2a) and

¹Yale University, Department of Molecular Biophysics and Biochemistry, 266 Whitney Avenue, P.O. Box 208114, New Haven, Connecticut 06520-8114, USA.

conventional fluorescence microscopy (Fig. 2b) showed that Nup53 overexpression led to the appearance of a distinctive Doa10–GFP signal that transected the nucleus in ~25% of the cells (Fig. 2f); the nuclei resembled the Greek letter theta (θ), so we refer to them as ‘theta nuclei’. A similar frequency of theta nuclei was observed when Nup53 was tagged with GFP (Fig. 2f). Neither the control vector nor *CUP1–NUP53 Δ C*, which fails to drive INM proliferation¹³, induced the appearance of theta nuclei (Fig. 2; Supplementary Fig. 4). We did not see theta nuclei in cells that overexpressed Hmg1 (HMG-CoA reductase), which induces ER lamellae around the outside of the nucleus (‘karmellae’)¹⁴ (Supplementary Fig. 4).

To validate the Nup53-based assay, we examined two proteins as controls: Sec61, an integral ER membrane protein that is found in intranuclear membranes in certain mammalian cells¹⁵, and Mga2, a membrane-anchored transcription factor precursor that is predicted to be excluded from the INM^{16,17}. Theta nuclei were seen with Sec61–GFP in ~25% of Nup53-overexpressing cells (Fig. 2c, f), but virtually no such nuclei were observed with Mga2–GFP (Fig. 2d, f). Therefore, the fluorescence assay provides a simple means for testing localization of membrane proteins to the INM, including those that also occupy the ER and outer envelope.

In contrast to Doa10, the other main transmembrane E3 of the yeast ER, Hrd1 (ref. 18), showed little if any localization to the INM (Fig. 2e, f), indicating that INM protein localization is highly selective. Three other proteins that function with Doa10—Ubc6, Ubc7 and Cue1—revealed frequencies of theta nuclei similar to Doa10–GFP (Fig. 2f). Doa10 is thought to form a membrane-embedded complex

with these proteins, and the localization data support the possibility that such a complex exists in the INM. Our results show that the Doa10 and Hrd1 E3 complexes concentrate in different subdomains within the continuous ER–nuclear envelope membrane system.

Role of the nuclear pore complex

Little is known about the transport of polytopic membrane proteins to the inner nuclear envelope. INM proteins are postulated to move from the ER through the lipid bilayer to the INM through lateral channels in the nuclear pore complex (NPC)^{19–21}. Initial evidence that the NPC might be involved in this process came from micro-injection of animal cells with antibodies or lectins that bind NPC subunits; this had modest and variable effects on INM localization of a model membrane protein²². To test the involvement of the NPC in INM transport and to gain insight into which components of the NPC are important for this, we examined Doa10–GFP by the Nup53-based assay in a panel of nucleoporin mutants (Fig. 2g). Importantly, deletion of two specific nucleoporins, Pom152 and Nup188, partially but significantly reduced the formation of theta nuclei. This was not due to inhibition of the import of Nup53, as Nup53–GFP showed normal frequencies of theta nuclei in *pom152 Δ* and *nup188 Δ* mutants (Fig. 2f). As expected, theta nuclei were almost never observed in *nup170 Δ* cells (Fig. 2g) because Nup170 is required for nuclear import of Nup53 (ref. 13).

Pom152 is an integral membrane protein, and it therefore could be in close proximity to, or a component of, the NPC lateral channels. Moreover, Pom152 directly binds Nup188, and a *pom152 Δ nup188 Δ* double mutation is lethal^{20,23,24}. The most straightforward interpretation of our data is that Nup188 and Pom152 form part of an NPC structure that is needed for efficient membrane protein movement through the NPC. If INM localization of Doa10 is necessary for efficient targeting of its nuclear substrates, the reduction in INM-localized Doa10, albeit modest, might lead to detectable defects in nuclear protein degradation. Indeed, degradation of *Deg1*– β gal, a nuclear substrate of Doa10, was moderately but significantly

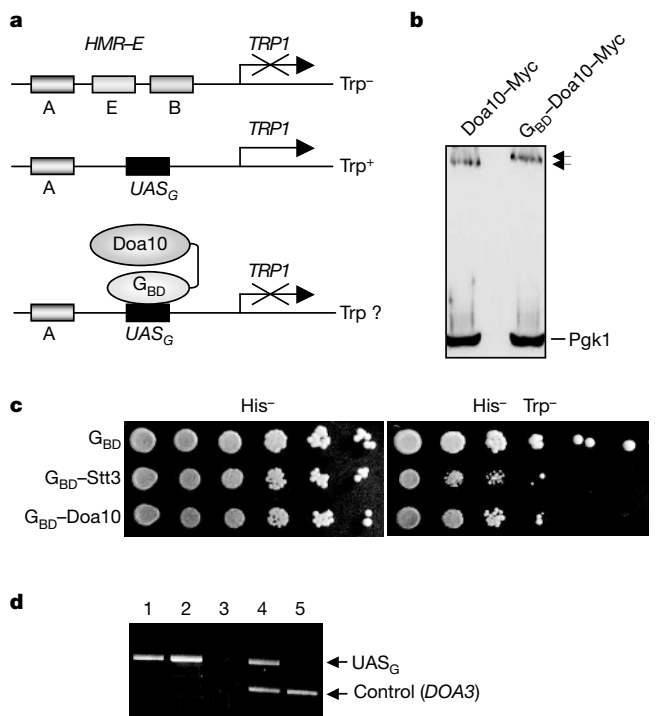


Figure 1 | Localization of a transmembrane ubiquitin ligase to the inner nuclear envelope. **a**, Targeted-silencing assay. In wild-type cells, *hmr::TRP1* is repressed (Trp^-). With a triplicated *UAS_G* replacing the E and B sites of the silencer (*Aeb::UAS_G::TRP1*; strain YSB35), silencing is lost (Trp^+). Introducing a *G_{BD}*–membrane protein fusion restores silencing if the protein can anchor the locus to the inner nuclear envelope¹¹. **b**, *G_{BD}*–Doa10–Myc expression is similar to chromosomal Doa10–Myc expression. Pgk1 is a 45-kDa globular protein. **c**, Targeted silencing by *G_{BD}*–Doa10 assayed with serially diluted YSB35 cells on drop-out plates lacking histidine (for plasmid selection) or both histidine and tryptophan. *G_{BD}*–Stt3 is the positive control. **d**, Chromatin immunoprecipitation analysis of *G_{BD}*–Doa10 binding to *UAS_G* in YSB35 (lanes 1–4) and YSB1 (no *UAS_G*, lane 5) cells. Anti-*G_{BD}* (lane 1), anti-Myc (lane 2) or no antibody (lane 3) was used. Lanes 4, 5: input extracts of YSB35 and YSB1 cells, respectively.

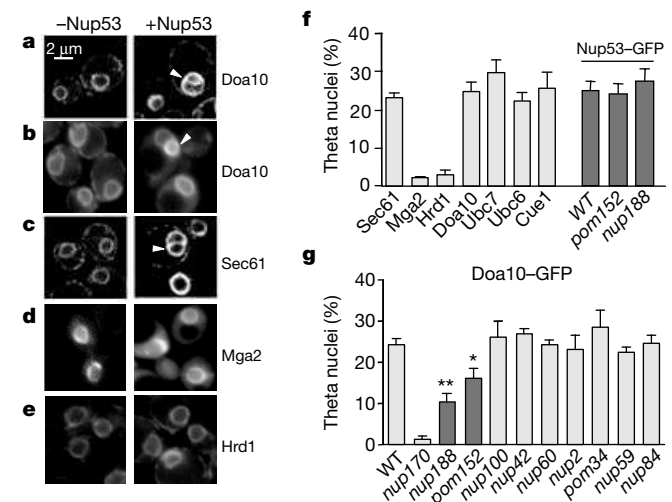


Figure 2 | Fluorescence assay of INM protein localization.

a–e, *pCUP1–NUP53* (right column) or vector (left column) was transformed into cells with chromosomally expressed GFP fusions to Doa10 (**a**, **b**), Sec61 (**c**) or Hrd1 (**e**), or into *ufd1-1* cells harboring a *GFP–Mga2* plasmid (**d**); the *ufd1-1* mutation prevents cleavage of latent Mga2 but does not affect INM trafficking. Cells were examined by confocal (**a**, **c**) or standard fluorescence microscopy (**b**, **d**, **e**). Arrowheads mark theta nuclei. **f**, Percentage of theta nuclei in cells expressing the indicated protein–GFP fusions. Error bars in **f**; standard deviation of three independent cultures. **g**, Doa10–GFP transport to the INM measured in nucleoporin deletion strains as percentage of theta nuclei. Double asterisk, $P < 0.001$ (relative to wild type, WT); single asterisk, $P < 0.01$.

impaired in *pom152Δ* and *nup188Δ* strains (Supplementary Fig. 5), although we cannot rule out indirect effects of the mutations.

Function of INM localization of Doa10

To test the inference that localization of Doa10 to the INM is functionally relevant, we tethered Doa10 to the cell periphery by fusing it to the actin-binding domain of coronin (Crn1) (Supplementary Fig. 6). Crn1 binds actin filaments and localizes to cortical actin patches²⁵. The first 400 residues of Crn1 were fused to the carboxy terminus of Doa10, followed by GFP; this *doa10-CNG* allele replaced the chromosomal *DOA10* gene. Doa10-CNG was expressed as a full-length protein (data not shown) and localized to foci that were primarily at the cell cortex (Fig. 3a), resembling the localization of native Crn1. Most importantly, Doa10-CNG failed to localize to the nuclear

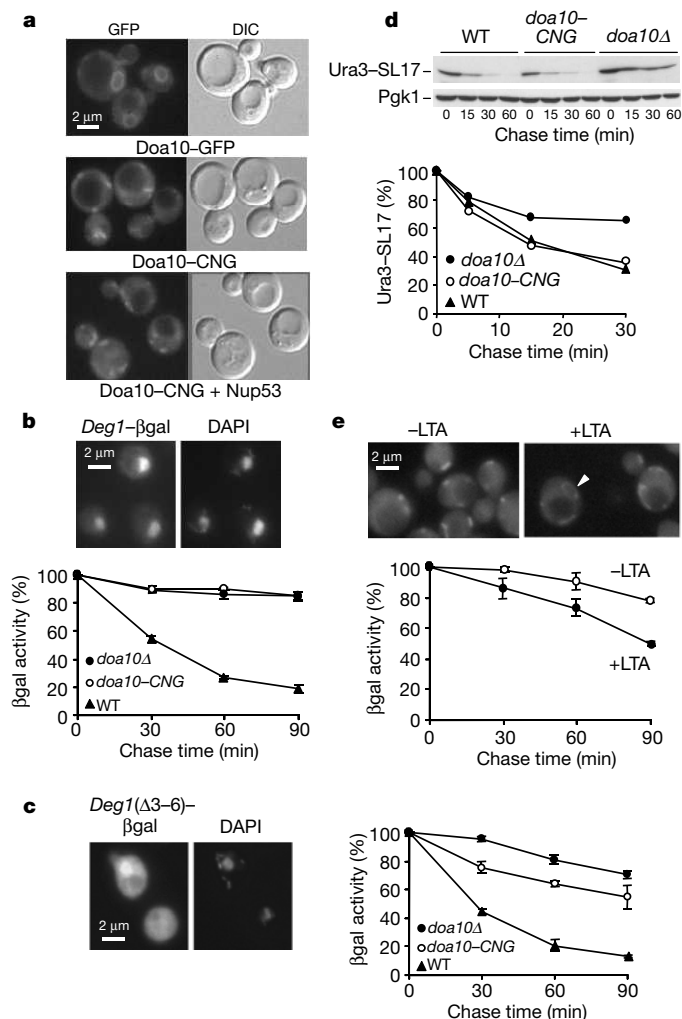


Figure 3 | Localization of Doa10 to the INM is required for nuclear substrate degradation. **a**, Doa10-CNG localizes to foci at the cell periphery; this is unaltered by Nup53 overexpression. **b**, Cytoplasmically tethered Doa10-CNG is inactive in nuclear *Deg1*-βgal degradation. Error bars in **b**, **c**, **e**: standard deviations of three independent measurements. Nuclear localization of *Deg1*-βgal was confirmed by anti-βgal immunofluorescence (top). **c**, The *Deg1*(Δ3-6)-βgal mutant is partially impaired in nuclear localization, which correlates with enhanced degradation in *doa10-CNG* cells relative to *doa10Δ* ($P < 0.05$). **d**, A soluble cytoplasmic substrate is degraded normally in *doa10-CNG* cells by cycloheximide-chase/immunoblot (upper panel) and standard pulse-chase (lower panel) analyses of the cytoplasmic HA-tagged Ura3-SL17 substrate. **e**, LTA treatment partially restores localization to the nuclear envelope and nuclear substrate degradation. *doa10-CNG* cells were treated with DMSO or 100 μM LTA. Arrowhead indicates nuclear envelope localization. Degradation of *Deg1*-βgal was significantly enhanced in LTA-treated cells ($P < 0.01$).

envelope and did not form theta nuclei when Nup53 was overexpressed. Proteolysis of the nuclear Doa10 substrate *Deg1*-βgal was severely impaired in *doa10-CNG* cells (Fig. 3b). The *doa10-CNG* allele did not cause a general ER stress response or defects in ER-associated degradation as measured by a *UPRE-lacZ* reporter assay and degradation of the misfolded ER substrate carboxypeptidase Y (CPY*) (data not shown).

When the nuclear localization signal (NLS) in *Deg1* was mutated²⁶, a substantial fraction of the resulting *Deg1*(Δ3-6)-βgal protein localized to the cytoplasm (Fig. 3c). A corresponding increase in degradation of *Deg1*(Δ3-6)-βgal was observed in *doa10-CNG* cells compared with *doa10Δ* cells. These results support the idea that cytoplasmically tethered Doa10 is at least partially functional but cannot access nuclear-localized substrate. Consistent with this, degradation of a Doa10 substrate that is almost exclusively cytoplasmic, Ura3-SL17 (ref. 9), occurred at wild-type rates when measured either by cycloheximide-chase/immunoblot (Fig. 3d, top) or pulse-chase analysis (bottom). Therefore, Doa10-CNG is functional against soluble cytosolic substrates but not nuclear ones.

When *doa10-CNG* cells were treated with latrunculin-A (LTA), an actin filament assembly inhibitor²⁵, actin patches disassembled within 5 min (not shown). Relocalization of Doa10-CNG from cortical sites to the nuclear envelope was much slower and incomplete, either because Doa10-CNG localization was stabilized by additional cortical interactions or because the Doa10-Crn1 fusion tended to aggregate²⁷. Nevertheless, we detected a weak nuclear rim signal with Doa10-CNG in ~20% of cells after 2.5 h in LTA (Fig. 3e). Importantly, in parallel with this partial restoration of localization to the nuclear envelope, we observed a statistically significant recovery of *Deg1*-βgal degradation (Fig. 3e).

Ubiquitin modification of the naturally short-lived Matα2 repressor occurs through two pathways, one that depends on Ubc6-Ubc7-Doa10, and the other on Ubc4 (refs 6, 8). Matα2 proteolysis was inhibited around threefold in both *doa10-CNG* and *doa10Δ* cells, indicating that nucleus-excluded Doa10-CNG is not active against Matα2 (Fig. 4a). Similarly, in both *doa10Δ ubc4Δ* and *doa10-CNG ubc4Δ* double mutants, Matα2 had the same half-life (~53 min), confirming that Doa10-CNG was not active against MATα2. Notably, partial restoration by LTA of Doa10-CNG localization at the nuclear envelope was associated with partial but significant suppression of the Matα2 degradation defect ($t_{1/2} \approx 30$ min; Fig. 4b). This was true even though LTA slightly inhibited Matα2 turnover in wild-type cells. We conclude that localization of Doa10 to the inner nuclear envelope is required for efficient targeting of a natural nuclear substrate.

Determinants of Doa10 INM localization

To address whether Doa10 contains specific INM-targeting sequences, we made complementary deletions, which removed either C-terminal residues 951-1319 (Doa10-N) or N-terminal residues 2-950 (Doa10-C), and performed theta-nuclei assays on the resulting GFP fusion proteins. Both proteins localized normally to the INM, indicating that Doa10 does not bear one unique INM-targeting or retention signal (Fig. 4c). However, it might carry two or more redundant signals.

Doa10 might be able to diffuse into the INM because it lacks any cytoplasmic loops larger than ~24 kDa. By contrast, the Hrd1 C-terminal cytoplasmic domain is ~38 kDa in size, and this might not allow passage through the NPC lateral channels²¹. However, fusion of the Hrd1 cytoplasmic domain to Doa10 did not block INM accumulation (Fig. 4c), indicating that the exclusion of Hrd1 from the INM depends on its membrane domain. Attachment of a larger globular protein, Pgc1 (~45 kDa), to Doa10 did significantly attenuate INM localization (Fig. 4c), consistent with a size limit that restricts diffusion through the NPC. The ability of these Doa10 fusion proteins to access the INM correlated with their ability to support degradation of Doa10 nuclear substrates (Supplementary Fig. 7a),

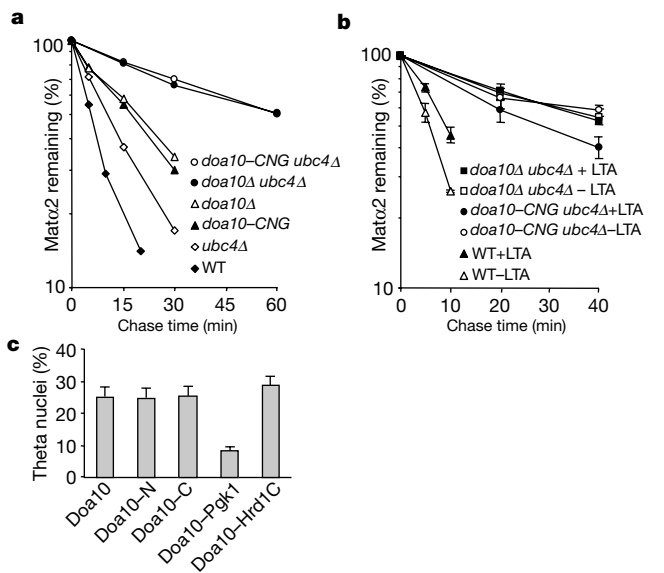


Figure 4 | Nuclear substrate degradation and determinants of Doa10 INM localization. **a**, Pulse-chase analysis of Mat α 2 degradation. Calculated half-lives of Mat α 2 were 6, 13, 19, 19, 52 and 53 min in wild-type, *ubc4 Δ , *doa10 Δ , *doa10-CNG, *doa10-CNG *ubc4 Δ and *doa10 Δ *ubc4 Δ cells, respectively. **b**, Partial recovery of Mat α 2 degradation through LTA treatment. Error bars in **b**, **c**: standard deviation of three independent cultures. LTA treatment of *doa10-CNG *ubc4 Δ cells significantly increased Mat α 2 degradation rates ($P < 0.05$) even though LTA impaired degradation in wild-type (WT) cells 1.7-fold ($P < 0.01$). **c**, Effects of Doa10 deletions and protein-domain fusions on Doa10 movement to the INM.*********

whereas degradation of cytosolic substrates was minimally affected by either fusion protein (Supplementary Fig. 7b).

The spatial regulation of ubiquitin system enzymes is increasingly recognized as a key aspect of their substrate specificity⁵. We have shown here that the selective localization of a transmembrane E3 complex to the INM is required for degradation of its nuclear substrates. This is the first example of a polytopic ER–nuclear envelope enzyme whose enzyme activity has been shown to be required in the nucleus. Spatial control of ubiquitin conjugation in the nucleus might be intricate. There is evidence for controlled movement of specific proteins and chromosomal loci to the nuclear periphery in both yeast and higher cells^{28–30}. Localization of a ubiquitin ligase to the inner nuclear envelope would allow it to transfer ubiquitin to chromosomal and nuclear proteins specifically when they move to the nuclear periphery. This provides a potential mechanism for the temporal and spatial regulation of transcription and other nuclear processes by ubiquitin modification.

Note added in proof: A very recent study³⁴ reported a pathway for INM trafficking of two related yeast transmembrane proteins that concentrate in the INM. This pathway is NLS-dependent and requires the Nup2 nucleoporin but not Nup188 or Pom152. In contrast, Doa10 has no obvious NLS, and its trafficking to the INM depends on Nup188 and Pom152 but not Nup2. These findings indicate that there are multiple pathways for integral membrane protein trafficking to the INM. For a protein such as Doa10, which is also needed in the ER, a pathway that strongly concentrates it in the INM should not be favoured.

METHODS

Yeast media and methods. Cells were grown at 30 °C in either rich (YPD) or selective minimal media. Yeast *hmr::TRP1* silencing assays were done by spotting tenfold serial dilutions of overnight cultures onto selective plates. The G_{BD} fusion alleles were carried on plasmids that also had a *HIS3* marker³¹. Growth was assessed after two days at 30 °C. For assays of theta-nuclei formation, induction of Nup53 was achieved by growing cells carrying the *CUP1-NUP53* plasmid in selective medium in the presence of 100 μ M copper sulphate for 16 h (ref. 13).

Degradation assays. Cycloheximide-chase/immunoblot analysis to follow Ura3–SL17 (haemagglutinin (HA)-epitope tagged) degradation was performed by growing strains to optical density at 600 nm (OD₆₀₀) ~1 in selective medium containing 100 μ M CuSO₄ followed by addition of cycloheximide to 0.5 mg ml⁻¹. Culture aliquots (2 OD₆₀₀ equivalents) were removed at the desired time points. After incubating the aliquots in 100 μ M NaOH at room temperature for 5 min, cells were pelleted and resuspended in Laemmli SDS gel loading buffer and heated at 100 °C for 10 min. Immunoblotting was done with an anti-HA monoclonal antibody, 16B12 (Covance), and anti-Pgk1 (Molecular Probes) was added to provide a loading control. Pulse-chase experiments to measure the half-lives of Ura3–SL17 and Mat α 2 were performed as described previously⁸. Half-lives were calculated after phosphorimager quantitation. Quantitative activity-chase analyses of Deg1- β gal degradation were done by blocking protein synthesis with cycloheximide and measuring loss of β gal activity with ortho-nitrophenyl galactoside (ONPG) substrate³². For statistical comparison of degradation rates, half-lives were calculated by linear regression, and mean values were compared by unpaired *t*-tests (GraphPad InStat).

Immunoelectron microscopy. Electron microscopy (EM) was performed by the University of Colorado EM facility as described³³. Affinity-purified rabbit polyclonal antibody to GFP diluted 1:100 in blocking solution was followed by goat anti-rabbit secondary antibody conjugated to 15 nm colloidal gold (1:20 dilution in blocking buffer).

Received 30 June; accepted 15 August 2006.

- Hochstrasser, M. Ubiquitin-dependent protein degradation. *Annu. Rev. Genet.* **30**, 405–439 (1996).
- Hershko, A. & Ciechanover, A. The ubiquitin system. *Annu. Rev. Biochem.* **67**, 425–479 (1998).
- Pickart, C. M. & Eddins, M. J. Ubiquitin: structures, functions, mechanisms. *Biochim. Biophys. Acta* **1695**, 55–72 (2004).
- Varshavsky, A. Regulated protein degradation. *Trends Biochem. Sci.* **30**, 283–286 (2005).
- Pines, J. & Lindon, C. Proteolysis: anytime, any place, anywhere? *Nature Cell Biol.* **7**, 731–735 (2005).
- Swanson, R., Locher, M. & Hochstrasser, M. A conserved ubiquitin ligase of the nuclear envelope/endoplasmic reticulum that functions in both ER-associated and Mat α 2 repressor degradation. *Genes Dev.* **15**, 2660–2674 (2001).
- Kreft, S. G., Wang, L. & Hochstrasser, M. Membrane topology of the yeast endoplasmic reticulum-localized ubiquitin ligase Doa10 and comparison with its human ortholog TEB4 (MARCH-VI). *J. Biol. Chem.* **281**, 4646–4653 (2006).
- Chen, P., Johnson, P., Sommer, T., Jentsch, S. & Hochstrasser, M. Multiple ubiquitin-conjugating enzymes participate in the *in vivo* degradation of the yeast MAT α 2 repressor. *Cell* **74**, 357–369 (1993).
- Ravid, T., Kreft, S. G. & Hochstrasser, M. Membrane and soluble substrates of the Doa10 ubiquitin ligase are degraded by distinct pathways. *EMBO J.* **25**, 533–543 (2006).
- Johnson, P. R., Swanson, R., Rakhilina, L. & Hochstrasser, M. Degradation signal masking by heterodimerization of MAT α 2 and MAT α 1 blocks their mutual destruction by the ubiquitin-proteasome pathway. *Cell* **94**, 217–227 (1998).
- Andrulis, E. D., Neiman, A. M., Zappulla, D. C. & Sternglanz, R. Perinuclear localization of chromatin facilitates transcriptional silencing. *Nature* **394**, 592–595 (1998); erratum **395**, 525 (1998).
- Taddei, A., Hediger, F., Neumann, F. R. & Gasser, S. M. The function of nuclear architecture: a genetic approach. *Annu. Rev. Genet.* **38**, 305–345 (2004).
- Marelli, M., Lusk, C. P., Chan, H., Aitchison, J. D. & Wozniak, R. W. A link between the synthesis of nucleoporins and the biogenesis of the nuclear envelope. *J. Cell Biol.* **153**, 709–724 (2001).
- Wright, R., Basson, M., D’Ari, L. & Rine, J. Increased amounts of HMG-CoA reductase induce “karmellae”: a proliferation of stacked membrane pairs surrounding the yeast nucleus. *J. Cell Biol.* **107**, 101–114 (1988).
- Isaac, C., Pollard, J. W. & Meier, U. T. Intranuclear endoplasmic reticulum induced by Nopp140 mimics the nucleolar channel system of human endometrium. *J. Cell Sci.* **114**, 4253–4264 (2001).
- Hitchcock, A. L. *et al.* The conserved Npl4 protein complex mediates proteasome-dependent membrane-bound transcription factor activation. *Mol. Biol. Cell* **12**, 3226–3241 (2001).
- Rape, M. *et al.* Mobilization of processed, membrane-tethered SPT23 transcription factor by CDC48^{UFD1/NPL4}, a ubiquitin-selective chaperone. *Cell* **107**, 667–677 (2001).
- Hampton, R. Y. ER-associated degradation in protein quality control and cellular regulation. *Curr. Opin. Cell Biol.* **14**, 476–482 (2002).
- Hinshaw, J. E., Carragher, B. O. & Milligan, R. A. Architecture and design of the nuclear pore complex. *Cell* **69**, 1133–1141 (1992).
- Suntharalingam, M. & Wenthe, S. R. Peering through the pore: nuclear pore complex structure, assembly, and function. *Dev. Cell* **4**, 775–789 (2003).
- Worman, H. J. & Courvalin, J. C. The inner nuclear membrane. *J. Membr. Biol.* **177**, 1–11 (2000).

22. Ohba, T., Schirmer, E. C., Nishimoto, T. & Gerace, L. Energy- and temperature-dependent transport of integral proteins to the inner nuclear membrane via the nuclear pore. *J. Cell Biol.* **167**, 1051–1062 (2004).
23. Nehrbass, U., Rout, M. P., Maguire, S., Blobel, G. & Wozniak, R. W. The yeast nucleoporin Nup188p interacts genetically and physically with the core structures of the nuclear pore complex. *J. Cell Biol.* **133**, 1153–1162 (1996).
24. Damelin, M. & Silver, P. A. In situ analysis of spatial relationships between proteins of the nuclear pore complex. *Biophys. J.* **83**, 3626–3636 (2002).
25. Goode, B. L. *et al.* Coronin promotes the rapid assembly and cross-linking of actin filaments and may link the actin and microtubule cytoskeletons in yeast. *J. Cell Biol.* **144**, 83–98 (1999).
26. Hall, M. N., Hereford, L. & Herskowitz, I. Targeting of *E. coli* β -galactosidase to the nucleus in yeast. *Cell* **36**, 1057–1065 (1984).
27. Appleton, B. A., Wu, P. & Wiesmann, C. The crystal structure of murine coronin-1: a regulator of actin cytoskeletal dynamics in lymphocytes. *Structure* **14**, 87–96 (2006).
28. Ishii, K., Arib, G., Lin, C., Van Houwe, G. & Laemmli, U. K. Chromatin boundaries in budding yeast: the nuclear pore connection. *Cell* **109**, 551–562 (2002).
29. Casolari, J. M. *et al.* Genome-wide localization of the nuclear transport machinery couples transcriptional status and nuclear organization. *Cell* **117**, 427–439 (2004).
30. Brickner, J. H. & Walter, P. Gene recruitment of the activated *INO1* locus to the nuclear membrane. *PLoS Biol.* **2**, e342 (2004).
31. Ma, J. & Ptashne, M. A new class of yeast transcriptional activators. *Cell* **51**, 113–119 (1987).
32. Plemper, R. K., Bohmler, S., Bordallo, J., Sommer, T. & Wolf, D. H. Mutant analysis links the translocon and BiP to retrograde protein transport for ER degradation. *Nature* **388**, 891–895 (1997).
33. Giddings, T. H. Jr *et al.* Using rapid freeze and freeze-substitution for the preparation of yeast cells for electron microscopy and three-dimensional analysis. *Methods Cell Biol.* **67**, 27–42 (2001).
34. King, M. C., Lusk, C. P. & Blobel, G. Karyopherin-mediated import of integral inner nuclear membrane proteins. *Nature* **442**, 1003–1007 (2006).

Supplementary Information is linked to the online version of the paper at www.nature.com/nature.

Acknowledgements We thank R. Sternglanz and R. Wozniak for strains and plasmids, P. Crews for generously providing LTA, O. Kerscher for Supplementary Fig. 1, and J. Wu and J. Wolenski for advice on confocal microscopy. We are grateful to S. Kreft, A. Lewis and T. Ravid for comments on the manuscript. This work was supported by the NIH.

Author Contributions M.D. performed all the experiments, and M.D. and M.H. planned the experiments, performed the data analysis and wrote the paper.

Author Information Reprints and permissions information is available at www.nature.com/reprints. The authors declare no competing financial interests. Correspondence and requests for materials should be addressed to M.H. (mark.hochstrasser@yale.edu).